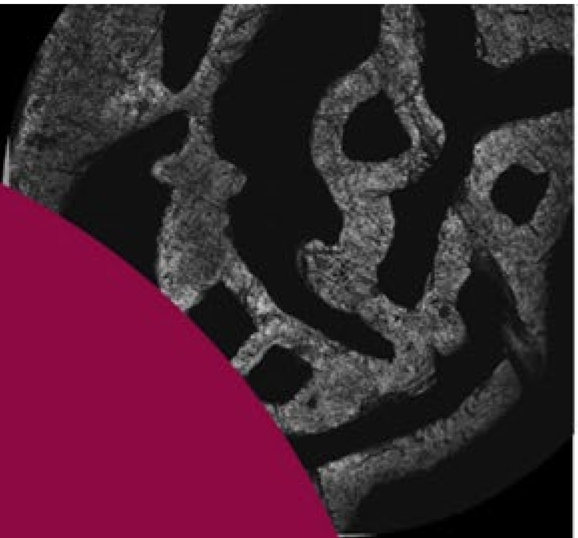

Arizona Imaging and Microanalysis Society

AIMS Poster Session

April 17, 2026

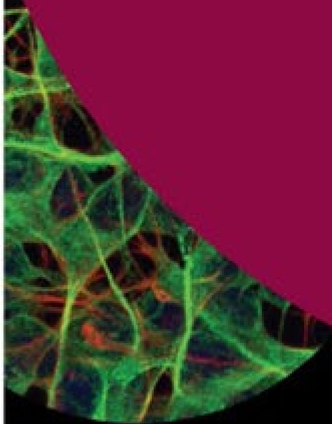

Arizona Imaging and
Microanalysis Society
azmicroscopy.org

2026 AIMS Conference

SCHEDULE

8:00 – 8:45 AM	**Check – In**
8:45 – 9:00 AM	**Opening Remarks**
9:00 – 9:40 AM	**Dewight Williams** *“Cryogenic Low Dose Imaging for Structure Determination”* **Eyring Materials Center, Arizona State University** (Research Scientist)
9:40 – 10:20 AM	**Katherine Jungjohann** *“Low Dose In-Situ and Multiscale Cryo Microscopy on Solid-Liquid Interfaces”* **National Laboratory of the Rockies** (Group Research Manager)
10:20 – 11:20 AM	**Morning Break/Student Posters/Visit Vendors**
11:20 – 12:00 AM	**Kedar Narayan** “ Volume Electron Microscopy: A Nanoscale Windo into 3D Cell Biology” **National Institutes of Health** (Group Leader – EM Core)
12:00 – 12:15 PM	**Microscopy Core Facilities in Arizona**
12:15 – 1:15 PM	**Lunch**
1:15 – 1:55 PM	**John Watts** *“Cryo-FIB/(S)TEM of Low-Z Hydrated, and Beam Sensitive Materials”* **Los Alamos National Laboratory, CINT** (Staff Scientist, Thrust Co-Leader)
1:55 – 2:35 PM	**Vendor Lightening Talks**
2:35 – 3:05 PM	**Break/Student Posters, final judging/ Visit Vendors**
3:05 – 3:45 PM	**Peter Ercius** *“Integrating Microscopy, Large Language Models, and Hight-Performance Computing”* **NCEM, Lawrence Berkeley National Laboratory** (Staff Scientist)
3:45 – 4:15 PM	**Jessica Warren** “*Developing a Microscopy Toolkit for the Cellular Biology of Non-Model and Intracellular Organisms”* **Arizona State University** (Postdoctoral Researcher)
4:15 – 4:45 PM	**Thomas Marchese** *“Hiding and Seeking Sodium Metal in Sodium Closo-Hydroborate, and Electron Beam Damage Study”* **University of Chicago** (NSF Graduate Research Fellow)
4:45 – 5:00 PM	**Awards and Closing Remarks**
5:15 – 5:40 PM	**AIMS Business Meeting** Annual Society General Meeting

TABLE OF CONTENTS

SPONSOR LIGHTENING TALKS

1:55-2:00 PM	**Dan Becker**, *West Sales Manager, Hitachi High-Tech America, Inc.* **Thinking Outside the Box-Making Cryo-TEM More Accessible**
2:00-2:05 PM	**Dominic Dominquez**, *Research Imaging Specialist, Nanoscience Instruments, Inc.* **Expanding Desktop SEM Capabilities: FEG Performance and True STEM Imaging with the Phenom Pharos**
2:05-2:10 PM	**Eliza Nieweglowska**, *Research Imaging Specialist, Thermofisher, Inc.* **Advancements in connected cryo-EM capabilities**
2:10-2:15 PM	**Michael Gray**, *Semiconductor Business Development Manager, Tescan* **Large Area Workflow for Semiconductor FA Incorporating s Novel Laser Ablation Technology and Plasma FIB SEM**
2:15-2:20 PM	**Adrian Peña**, *Microscopy Sales Representative, Evident Scientific/Olympus* **Research Imaging Technologies from Evident Scientific**
2:20-2:25 PM	**Steven Goodman**, *Chief Scientific Officer Microscopy Innovations LLC* **Automated Specimen Processing for Electron Microscopy with mPrep ASP Processors**

Poster Abstracts

[Grad] Analysis of Differential Whole Brain Neuronal Activation in Early vs Late Aversive Learning

Makenna Carges, Lindsay Halladay

In order for an animal to survive, the brain must be able to accurately recognize threats and respond with an appropriate defensive action. We use a mouse model of Pavlovian fear conditioning to investigate the details of this process. For this conditioning paradigm, mice are trained to fear an auditory tone by pairing it with a physical stimulus like a mild aversive foot shock. Throughout subsequent trials and further reinforcement of the tone-shock paradigm, the animal begins to respond with fear to the auditory tone, even when uncoupled to the shock. In mice, this fear response is freezing, a species-specific expression of fear. Several regions of the brain are thought to coordinate this complex process: the amygdala assigns negative valence to the tone predicting the aversive outcome of the shock, the hippocampus encodes contextual information relevant to the tone-shock outcome such as visual and olfactory input, and the prefrontal cortex mediates the selection of a defensive response to the tone-shock stimuli.

Our lab is investigating the role of the bed nucleus of the stria terminalis (BNST) in shifting an organism's focus from general situational fear to specific fear early in acquisition where the stimulus-outcome contingency shifts from uncertain to certain. Our lab is using a modified cued-fear learning paradigm to differentiate between uncertain and certain fear in the mouse. This protocol involves three groups of mice: a context control group, a 1xcs group, and a 5xcs group. The 1xcs group is placed in a fear box and experiences one tone-shock pairing. This animal goes through a single trial and therefore does not have the understanding that every shock is preceded by a tone. The 5xcs group undergoes 5 rounds of tone-shock pairing with ten minute inter trial intervals (ITIs). By the end of this protocol, the 5xcs animal understands that if it experiences a tone it will also experience a shock therefore develops a fear for the tone as the animals understands the shock will soon follow. The 5xcs animal builds an understanding that there is a clear and predictable nature to the threat, in this case the shock.

After performing the cued-fear learning protocol, we used a multiplex immunohistochemistry approach to stain for antigens related DAPI to evaluate neuronal cell bodies, Cfos to evaluate neuronal activation in the 90 minutes before brain collection, and retrograde fluorogold that gives us the ability to visualize neuronal connections into the BNST. This approach allows us to investigate how differences in neuronal encoding of uncertain vs. certain stimulus-outcome contingencies may differ. In performing this experiment, fluorescent imaging and qualitative analysis of paired sequential brain sections revealed broader activation of BNST projections to the basolateral amygdala (BLA) under the 5xcs disambiguous fear context. This differential activation points to a possible role for the BNST in modulating BLA activity in the process of fear acquisition.

[Grad] Structural Insights into the Rubisco–Rubisco Activase Complex in Higher Plants

Kira DeVore, Kazi Waheeda, Isabella Breen, Alexander Carsten, Rebekka Wachter, Po-Lin Chiu

Ribulose-1,5-bisphosphate carboxylase/oxygenase (Rubisco) catalyzes the first committed step of carbon fixation in photosynthesis, but its efficiency is limited by slow turnover, due to the non-specific O2/CO2 binding and the blockade of sugar phosphates. To sustain catalytic activity, plants employ Rubisco activase (Rca), a chaperone ATPase, that harnesses ATP hydrolysis to remodel Rubisco active site by engaging the N-terminal Rubisco large subunit (RbcL) and promoting the release of inhibitors. Despite its central role, the mechanistic basis of the Rubisco–Rca interaction remains unresolved due to the complex's dynamic and heterogeneous nature.

We are pursuing single-particle cryogenic electron microscopy (cryo-EM) to capture the Rubisco–Rca complex from higher plants, specifically Spinacia oleracea. Ongoing work focuses on optimizing protein purification, complex assembly, and EM sample preparation to stabilize and visualize this transient interaction. Preliminary data suggest that Rca assembles into higher-order oligomers and interacts with Rubisco in a transient, dynamic manner.

These efforts aim to obtain the first high-resolution and full-length structure of plant Rubisco engaged with Rca, providing mechanistic insight into how Rca restores Rubisco function to maintain carbon fixation. The outcome has broad implications for understanding photosynthetic regulation and guiding strategies to engineer crops with improved photosynthetic efficiency.

[Grad] **Structural basis for echinocandin inhibition of fungal glucan synthase**

Md Shamiul Islam, Darpan Raghav, Thomas M Tomasiak

The echinocandins are a widely used antifungal class of drugs that target the Fks1, the catalytic subunit responsible for fungal cell wall β-1,3-glucan synthesis and are essential for treating emerging fungal infections. We solved the cryo-EM structures of Fks1 at 3.0Å from Nakeomyces glabratus, a rapidly emerging fungal infection, and identified the mechanism of action for inhibition by the echinocandin caspofungin. Caspofungin binds in the transmembrane region near the membrane surface to an aromatic-rich region near the transport pathway and clinical hotspot mutants. A comparison to the apo structure shows that caspofungin displaces bound sterol molecules from the membrane-periplasm interface and allosterically induces a change along the lipid network outside the transmembrane domain that connects from its binding site to the catalytic domain. These results near three clinical resistance “hotspot” regions that cluster in this area, and the confluence of echinocandin binding and the catalytic and transport mechanisms.

[UG] **Fibroblast-Mediated Induction of Quiescence in HeLa Cervical Cancer Cells Under Oxidative Stress: Implications for Therapeutic Resistance and Tumor Relapse**

Jusreen Kaur, Bri Bryant, Benjamin Manus, Susan Holechek, PhD.

Tumor progression and therapeutic resistance are strongly influenced by interactions between cancer cells and the surrounding stromal microenvironment, particularly fibroblasts. This study investigates whether human fibroblasts can modulate oxidative stress responses in cancer cells, promoting survival through the induction of a reversible quiescent state rather than apoptosis. We hypothesize that under oxidative stress induced by hydrogen peroxide, MRC-5 subcutaneous fetal human lung fibroblasts will secrete stress-response mediators including cytokines, growth factors, and metabolic support factors that activate pro-survival signaling in HeLa cervical cancer cells to divert them from caspase-mediated apoptosis to a non-proliferative but reversible state. To test this, HeLa cells will be cultured alone and in co-culture with MRC-5 fibroblasts under conditions with and without oxidative stress. Parallel control groups will establish baseline responses for each cell type independently. Co-culture systems using removable inserts will allow assessment of both direct cell-cell interactions and indirect signaling. Following treatment, immunofluorescent staining for vimentin will distinguish fibroblasts from cancer cells, while cleaved Caspase-3 and Ki-67 staining will quantify apoptosis and proliferation, respectively. A reduction in apoptotic markers alongside decreased proliferation in HeLa cells would indicate a shift toward quiescence.

To isolate the effects of soluble factors, conditioned media from MRC-5 fibroblasts grown under normal and oxidative stress conditions will be applied to HeLa cultures. Comparative analysis will determine whether stress-induced secretions alone are sufficient to alter cancer cell fate. Finally, a reversibility assay will assess whether the non-proliferative state is transient (quiescence) or permanent (senescence) by monitoring the restoration of Ki-67 expression after removal of oxidative stress.

This research aims to model a more physiologically relevant tumor microenvironment and elucidate mechanisms by which fibroblasts contribute to cancer cell survival and treatment resistance. Understanding how stromal signaling promotes quiescence may provide insight into cancer relapse following chemotherapy and inform the development of more effective therapeutic strategies.

[Grad] **A pH-responsive probe for targeting the uniquely alkaline gut of mosquito larvae**

Emma Kempton, Thilini N. Thennakoon, Thomas Oldham, Michael Riehle, John C. Jewett**

Annually, more than 400,000 deaths are caused by mosquito-borne diseases, which emphasizes the need for new and effective vector control measures. Herein, we discuss a probe that targets the uniquely high pH conditions of the mosquito larval gut. This probe is referred to as Meldrum's acid amine-reactive Michael acceptor (or MaMa). This small-molecule probe selectively and irreversibly binds to lysine residues at high pH. It also allows for modular attachment of various functional cargoes, facilitating different applications such as fluorescent imaging, proteomics, and targeted toxicity. We have synthesized multiple variants of the probe and evaluated their biological applications using confocal microscopy, western blotting, and toxicity assays. Preliminary results have shown the probes' promise in imaging, proteomics, and as a potential larvicidal agent. My goal is to determine the capabilities of the MaMa probe for investigating the mosquito larval gut to expand our knowledge of the larval gut proteome and contribute to the development of new vector control strategies.

[PD] Cryo-EM reveals a novel antifungal transport mechanism driving drug resistance in Candidozyma auris

Darpan Raghav, Md. Shamiul Islam Rasel, Thomas Tomasiak

The rising threat of Candidozyma auris stems from its ability to withstand multiple medications, leading to life-threatening conditions for individuals with weakened immune systems. Its notable tolerance to azole antifungals emphasizes the need to better understand how this organism evades treatment at the molecular level. One of the primary contributors to this resistance is Candida drug resistance protein 1 (Cdr1), an ATP-binding cassette (ABC) transporter that removes antifungal agents from the cell, thereby reducing their effectiveness. Gaining detailed insight into how Cdr1 functions is key to identifying new ways to counteract resistance in C. auris. Here, we report the first Cryo-EM structures of C. auris Cdr1 in apo and fluconazole-bound states. Two fluconazole molecules were found within the protein's central cavity, with their binding largely stabilized by hydrophobic interactions. Using site-directed mutagenesis, we identified key amino acid residues that play a crucial role in fluconazole binding. Additionally, taking cues from human ABCG2, Cdr1 homologs from C. albicans and C. glabrata, and the yeast ABC transporter Pdr5, we engineered multiple Cdr1 variants by altering residues predicted to participate in substrate uptake, passage, and release. The functional impact of these mutations was assessed using yeast survival assays and Nile red transport assays to evaluate the substrate transport ability of the mutants. Together, results from Cryo EM, viability assays, transport measurements, fluorescence polarization studies, and molecular dynamics simulations identified key residues responsible for substrate recognition and efflux and support a peristaltic mode of transport in Cdr1 involving coordinated entry, gating, and release steps. These findings deepen insight into how Cdr1 drives azole resistance in C. auris and establish a basis for designing new antifungal therapies that can target this transporter to overcome drug resistance.

[Grad] Spatially resolved moiré exciton fine structure using cryogenic low loss EELS

Sriram Sankar, Patrick Hays, Medha Dandu, Mit H. Naik, Elyse Barre, Takashi Taniguchi, Kenji Watanabe, Steven Louie, Felipe da Jornada, Sefaattin Tongay, Jordan Hachtel, Peter Ercius, Archana Raja, and Sandhya Susarla

Moiré systems provide a powerful route to tune the electronic properties of transition metal dichalcogenides (TMDs) through the twist degree of freedom. These structures enable the creation of periodic, spatially localized quantum potentials, offering exciting possibilities for quantum technologies. In twisted TMDs, excitons (electron–hole pairs) are predicted to localize within the moiré potential. Optical spectroscopy has revealed twist-dependent modifications of both interlayer and intralayer excitons at cryogenic temperatures. However, the lack of sufficient spatial resolution makes it challenging to directly determine where these excitons are localized.

High-angle annular dark-field (HAADF) scanning transmission electron microscopy (STEM), combined with low-loss electron energy loss spectroscopy (EELS), provides a means to probe excitonic behavior with high spatial resolution by accessing the imaginary part of the dielectric function, which reflects the excitonic density of states. Despite this potential, such experiments are technically demanding due to limitations in monochromator

resolution, detector sensitivity, and cryogenic stability. Previous studies on R-stacked WS_2/WSe_2 heterostructures have shown that in-plane structural reconstruction occurs due to variations in local stacking configurations (AA, AB, and BA), with excitons preferentially localized in AA regions. However, limited energy resolution (%100 meV) and low signal-to-noise ratio have prevented the resolution of fine excitonic features.
Recent advances in monochromator technology now enable energy resolutions below 10 meV. In this work, a Nion Hermes microscope with a sub-nanometer probe and %15 meV energy resolution is used to investigate low-loss excitations in 1.9° twisted WS_2/WSe_2 moiré heterostructures. Fast, aberration-corrected medium-angle annular dark-field (MAADF) STEM imaging is performed simultaneously with low-loss EELS spectrum imaging to visualize the moiré pattern while minimizing beam damage. A custom Python-based workflow is implemented to perform cross-correlation-based drift correction and zero-loss peak alignment, reducing the four-dimensional dataset into an analyzable three-dimensional form.

The spatially averaged EELS spectra reveal a subtle shoulder feature in addition to the main excitonic peaks. Further analysis of spectra from distinct stacking regions (AA, AB, and BA) shows measurable variations in the low-loss response. These observations suggest sensitivity to local structural and electronic variations within the moiré lattice. Ongoing work focuses on correlating these spectral differences with local heterogeneities to gain a deeper understanding of exciton behavior in twisted TMD systems.

[Grad] **CryoEM analysis of the MCT4-CD147 transporter complex**

Annika K. Schulz, Devin J. Seka, Tarjani M. Thaker, Thomas M. Tomasiak

The proton and lactate cotransport activity of MCT1 & 4 (monocarboxylate transporters 1 and 4) fuels malignancy in a wide range of cancers. MCT4 is also implicated in pulmonary fibrosis. Therefore, the inhibition of these solute carrier class proteins has been the focus of many studies. Many MCT-targeting inhibitors have been developed and studied, however, there are no currently FDA-approved inhibitors targeting MCT4, due to a lack of knowledge on protein-drug selectivity. Here, we present two novel cryoEM structures of MCT4-CD147, one apo and one drug bound. Based on these structures, we have drawn conclusions about MCT4's conformational landscape and drug binding that finally give insight into its selectivity and ability to be inhibited.

[Grad] **Probing Phonons Induced by Polarization using Differential Momentum Resolved Scanning Transmission Electron Microscopy-Electron Energy Loss Spectroscopy**

Mahir Manna, Shayantan Chaudhury, Surya Prakash Reddy, Sujit Das, Katherine Inzani, Jan Rusz, Sandhya Susarla

Thin film proper ferroelectrics such as PbTiO3 have broken inversion symmetry that exhibits spontaneous polarization at room temperature. The behavior of polarization has been well studied using HAADF-STEM imaging, Four-Dimensional Scanning Transmission Electron Microscopy (4D-STEM). An aspect that has not been largely explored is the relationship between phonons and polarization in ferroelectrics. At atomic scale level the behavior of phonon mode is still unknown. The conventional methods to study phonons such as Raman spectroscopy, infrared spectroscopy have a spatial resolution of 1 µm and depth resolution of more than 100 nm, which is not enough to phonon modes at domains and domain walls. This limitation can be overcome by vibrational Electron Energy Loss Spectroscopy (vib-EELS) technique in STEM, which provides spatial resolution of 1 Angstrom as well as energy resolution below 10 meV. Off-axis EELS technique enables to collect spectra at different scattering angles in momentum space, avoiding the forwardly scattered phonons. This technique has been employed to look at non-ferroelectric materials with mapping phonons. In ferroelectric materials it is still a challenge due to the unknown relationship between inelastic and elastic scattering. We developed a new technique called differential momentum resolved off-axis STEM-EELS that can exclusively map out the phonons due to polarization vectors. The inspiration behind differential momentum resolved off-axis STEM-EELS comes from breaking Friedel's Law, which results in differential scattering in the polar directions in the momentum space due to multiple scattering effects. The idea behind the diff-q STEM EELS is to park the electron beam at polar and non-polar direction in the q-space and collect phonon spectra from those positions. We use PbTiO3 grown on DyScO3 as our model system which hosts “c” and “a” type of domains separated by a 90-degree domain wall. We implemented diff-q STEM-EELS technique , on a monochromated NION USTEM at the Eyring Material Center in Arizona State University. The spectra were collected from c domain in a prototypical thin film PbTiO3 grown on DyScO3 substrate. In c domain the [001]pc direction is perpendicular to the thin film-substrate interface whereas in a domain the [001]pc direction is parallel. To go to off-axis mode, we displaced the central diffraction spot away from EELS entrance aperture by an amount of 40 mrad to four spots along [001] and [100] direction in q-space. The microscope was operated at 60 keV and a convergence angle and a collection angle of 19 mrad was used for the experiment. Point spectra were collected from 11 different points from c domain with an exposure time 500 second for each spectrum. The background subtraction was performed by using a custom-made Gaussian-Lorentzian fitting. The results show a significant difference in the spectra between spot 1,2 (conjugate pair along [001]) and spot 3,4 (conjugate pair along [100]) in c domain. The phonon mode at ~ 37 meV along [100] direction got suppressed compared to [001] direction. The peak near 100 meV was observed more intense at spot 2 compared to spot 1and at spot 3 compared to spot 4.

[Grad] Integration of Imaging and Quantitative Analysis in an Immersive Wound Healing Curriculum for Online Learners

Benjamin Manus, Ayden Hall, Susan A. Holechek

Immersive, research-driven learning experiences provide an effective framework for developing both technical and analytical skills in cell biotechnology. The intensive Research Immersion Week, offered by the School of Life Sciences at ASU and supported by the SOLUR Catalyst Grant, is designed to provide hands-on research and wet-lab experience for both online undergraduate and graduate students. Participants of the Spring 2026 cohort investigated dermal wound healing using an in vitro co-culture model of fibroblasts and keratinocytes, with a strong emphasis on fluorescence and brightfield microscopy and image-based analysis. This semester was focused on understanding the molecular mechanisms of wound healing while also learning different assay techniques commonly used in cell and molecular biology.

Students generated high-resolution, multi-channel fluorescence images through immunocytochemistry (ICC), targeting markers such as Ki67, cytokeratin, and vimentin alongside cytoskeletal and nuclear staining. Instruction focused on proper fixation techniques, image acquisition, and minimizing background. A major component of the curriculum involved quantitative image analysis using software platforms such as QuPath for both fluorescence and brightfield images. These analysis techniques were integrated with other molecular biology assays, including brightfield scratch assays and RT-qPCR, enabling students to correlate spatial protein localization and cytoskeletal organization with gene expression and cellular behavior. Emphasis was placed on the interpretation of quantitative outputs.

The Immersion Week model fostered increased student proficiency in microscopy techniques and image analysis, as well as improved ability to extract biologically meaningful insights from complex datasets. This approach underscores how integrating advanced imaging and quantitative analysis into intensive laboratory experiences enables students to translate technical skills into meaningful scientific insight. This immersion program allowed the opportunity for the online student community to gain valuable hands-on experience learning wet lab techniques and engaging in focused research in a manner that is not usually available to them.

[Grad] Wrapping glial cells are needed for peripheral axon survival

Shree Narasimhan, Megan Corty

Around 70% of the human peripheral nervous system consists of unmyelinated fibers ensheathed by glial cells called Remak Schwann cells (Remaks) yet, the function of these glial cells in supporting neurons is still unclear. This is especially important when thinking in the context of peripheral nerve diseases. Unfortunately, the research gap in this topic stems from a lack of robust research tools in studying Remak cells directly. However, a good alternative in studying Remaks is to study wrapping glial cells found in Drosophila melanogaster (fruit flies) because wrapping glial cell ensheathment is similar to Remak-like ensheathment. Our lab focuses on how wrapping glia aid in axon survival mechanisms. We utilize flies that have certain pro-death genes knocked out in their genotype and compare the survival of axons when wrapping glia are present as well as when they are ablated. We observed that in flies that had the wrapping glia ablated, an axotomy led to axon death irrespective of whether the fly had pro-death genes knocked out or not. Our work identifies a previously unexplored role of wrapping glia in axon survival which can have broader implications in peripheral health and disease.

[UG] **BNST Circuits in Cued Fear Learning**

Olanma Ogbonnaya, Lindsay Halladay

Post-traumatic stress disorder, along with other anxiety disorders, are characterized by overgeneralization of fearful stimuli, leading to inappropriate behavioral reactions and reactivation of fearful memories in the absence of threat. Understanding the neural mechanisms underlying the recollection of fear memory is integral to improving treatments for anxiety and trauma-related disorders.

Using a rodent model (CRB6(Cg)-Crhtm1(cre)Zjh/J), we used in vivo electrophysiological recordings and chemogenetic manipulation to examine the roles of somatostatin-expressing (SST) and corticotropin-releasing factor–expressing (CRF) neurons within the BNST. Mice underwent cued fear conditioning with presentations of either one or five tone-shock pairings. This acquisition was followed by a recall test 24 hours later. Using in vivo single-unit recordings, we classified units in the bed nucleus of the stria terminalis (BNST) based on dynamic signaling properties during fear learning. 'Phasic' units increased firing rates after early, but not late, tone-shock pairings, while 'ramping' units gradually increased firing rates across the session. We also manipulated somatostatin-expressing (SST) or corticotropin-releasing factor-expressing (CRF) BNST neurons during fear conditioning to explore their roles in fear learning.

To confirm whether the BNST had been correctly targeted by the virus and to aid interpretation of the virus's behavior and the results from behavioral and electrophysiological experiments, the brains of sacrificed mice were examined by fluorescence microscopy (cellSens, Olympus). Coronal brain slices were analyzed at 10x magnification to assess the pattern of viral expression, its anterior and posterior diffusion, fluorescence intensity, and its position relative to the BNST.

To better understand the afferent innervation of the BNST, retrograde tracing studies were performed on a rodent model (C57BL/6 mice) using FluoroGold and FluoroRuby injection in the BNST. After successful tracer staining, IHC was performed to detect tracer-stained neurons and co-localize them with c-Fos, an index of activated neurons during fear memory retrieval. The fluorescence microscopic images (cellSens, Olympus) were analyzed at 20x magnification to determine the distribution patterns of tracer-stained neurons and to elucidate the brain regions that project to the BNST, as well as whether these connections are involved in fear memory retrieval.

[UG] **Matrix Metalloproteinase-1 is Required for Peripheral Nerve Wrapping**

Bryce A Rosen, Megan M Corty

Glial cells are essential components of the nervous system but remain understudied. Particularly, all peripheral nerves are wrapped by specialized glial cells in either a myelinating or non-myelinating fashion. Despite comprising nearly 70% of peripheral nerve wrapping, non-myelinating Remak Schwann Cells have remained poorly understood. Here, using the analogous Drosophila Wrapping Glia, we have identified Matrix Metalloproteinase-1 to be involved in proper wrapping development. Using confocal microscopy, wrapping analysis in both MMP-1 knockdown, enzymatic inhibition, and partial knockout conditions have demonstrated altered wrapping phenotypes, demonstrating its necessary role in wrapping development. These results deepen our molecular understanding of wrapping development and open an avenue to investigate potential upstream regulators of MMP activity as it relates to wrapping development.

[UG] **Identifying Genes Required for Wrapping Genes Development and Function**

Zachary Boydell, Ellie Schrock, Megan Corty

Within the peripheral nervous system, all axons are ensheathed by glial cells. This ensheathment can provide insulation to axons, increasing speed of neural transmission. Additionally, these axon-associated glial cells are believed to be important for providing nourishment and other support to neurons, because loss of ensheathment or genetic mutations affecting glial-expressed genes can lead to neurodegeneration. Despite these observations, the exact molecular nature of how ensheathment develops and precisely how these glial cells support neurons remain poorly understood. We study specialized glia termed wrapping glia in Drosophila melanogaster as a useful model to identify the molecular pathways important for the Development and function of axon-ensheathing glia. Using cell-type specific RNAi mediated gene knockdown, we were able to knockdown genes specifically in wrapping glia to assess the effects on development by examining wrapping glial morphology in Drosophila larvae. We screened genes associated with the TGF- Beta signaling pathway, such as baboon (babo) and screw (scw), and genes that regulate cell cycle progression and division such as Cyclin A (CycA) and the Origin recognition complex subunit 2 (ORC2). In a separate set of experiments to better understand how wrapping glia support the long-term health of neurons, we followed-up on several genes previously identified in a screen for glial genes required for support of injured neurons, now studying them in a natural aging paradigm. Specifically, we knock down the genes, Ddr, Mp, Mmp1, and babo in wrapping glia and then assay for neurodegeneration in uninjured aged flies at 4, 14, and 28 days after eclosion. These experiments are still ongoing. Overall our work to identify genes that are required for glial development and glial support is an essential first step that will ultimately allow us to determine how to harness glial support mechanisms to preserve neuronal function after injury or in disease.

[Grad] Multiple textures of FRIGN zircon at the nanoscale

Leah Shteynman, Thomas G. Sharp

Shocked zircon microstructures have the potential to yield information about the conditions of impact, including pressure, temperature, and time. One microstructure, granular zircon with non-random crystallographic, has been widely documented at impact structures on Earth. Two mechanisms have been proposed in the literature for the formation of this microstructure: (1) transformation to and back from a high-pressure zircon polymorph, and (2) decomposition to immiscible silica-rich liquid and zirconia, followed by nucleation of zircon neoblasts. Two granular zircon grains from the Chassenon suevitic breccia at Rochechouart impact structure were investigated by SEM/TEM/STEM to constrain their mechanism(s) of formation.

A Zeiss Auriga FIB/SEM at Arizona State University (ASU) was used for EBSD. A Helios 5UX dual beam FIB/SEM at ASU was used to section and thin samples. These samples were analyzed using a Talos f200i TEM/STEM at ASU. Analysis included TEM and STEM imaging, diffraction, and elemental mapping with EDX.

Both grains are polycrystalline, show the FRIGN orientation relationship, and have one predominant crystallographic orientation with two sub-dominant ones. Grain A is made up of zircon crystallites 0.2-1.6 µm, with domains of similarly sized granules, and overall size gradation across the grain. Perpendicular to the direction of size gradation there is some elongation of granules. Twinned reidite granules (0.8-2.6 µm) occur in the grain interior. Grain B granules are 0.5-1.2 µm, and granule size distribution is heterogeneous. Overall, from EBSD analysis, these grains appear quite similar. Bright-field TEM from Grain A shows it is made up of %200 nm crystallites, with minor areas of interstitial zirconia nanocrystals surrounded by amorphous silica, aligned in a planar fabric. Grain boundaries are complex, and granules are moderately strained. Grain B shows two distinct textural regions. At one end of the foil, highly rounded granules range from 350-500nm and contain large numbers of randomly distributed crystalline zirconia and amorphous silica crystallites. These granules have complex boundaries: a clear, sharp internal boundary surrounding most of the granule, a layer of porous nanocrystalline zircon outside of that, and a poorly defined irregular exterior boundary. In most areas the granules are connected by the porous zircon. Triple junctions replaced by voids are common in this region. The other texture consists of relatively inclusion-free granules with tight boundaries, low strain, a planar fabric, and no interstitial voids. Where inclusions do exist, they follow granule boundaries with the porous texture and do not contact granule boundaries. The silica inclusions are concentrically interior to zirconia inclusions. In both regions, most granules have low strain, but a small number of granules have very high strain.

Grain A is consistent with a zircon ⍰ reidite ⍰ zircon pathway. Grain B's inclusion-poor regions are likely back-transformed reidite lamellae. Transformation to and from reidite would have removed the high concentration of defects introduced by shock. Grain B's inclusion-poor regions are likely zircon that never transformed to reidite. If zircon was shocked but never transformed to reidite, there would have been a high concentration of defects, which could have been nucleation sites for decomposition products.

[UG] Investigating the Effects of Early Life Stress on Social Behavior and Neural Encoding

Sawyer Sullivan, Janet Ronquillo, Sriparna Majumdar, Lindsay Halladay

Exposure to early life stress (ELS) can lead to lifelong dysregulation of neural stress systems and incite lasting behavioral deficits. Our lab uses a mouse model of childhood neglect, maternal separation with early weaning (MSEW), which reliably produces neural and behavioral effects that mimic childhood adversity. Additionally, we are focusing on the inheritance of the effects of ELS, in offspring that have never been exposed to the stressors. In these studies, we explored how ELS affects both social behavior and neural activation in stress-related pathways. We are particularly interested in the neural projection from the bed nucleus of the stria terminalis (BNST) to the paraventricular nucleus (PVN), a pathway that normally activates the body's stress response system and thereby is crucial for stress regulation. Following exposure to MSEW, we assessed ELS effects on social behavior using an established assay that tests social motivation and novelty preference in two phases. Phase 1 tests social motivation as subjects interact with either an object or a conspecific. Phase 2 tests novelty preference, where subjects interact with either a familiar or an unfamiliar conspecific. MSEW resulted in social motivation deficits relative to controls. Following behavior, we immunolabeled neurons that are activated by social behavior and stressors and found that MSEW altered the neural encoding of both stress and socialization. Current investigations in our lab are also assessing how the effects of ELS are intergenerationally transmitted to offspring.

[Grad] Semantic Segmentation Convolutional Neural Network (CNN)

Mai Tan, and Peter Crozier

The Oxygen Exchange Reaction (OER) on the surface of nonstoichiometric oxides, such as ceria, is driven by the dynamic creation and annihilation of oxygen vacancies. Understanding these atomic-level variations is critical for optimizing material performance in applications like oxygen sensors and solid oxide fuel cells. However, quantifying atomic column occupancy and oxygen transport paths from in-situ Transmission Electron Microscope (TEM) images remains a significant challenge due to inherent image noise and the inherent limitations of 2D projections of phase contrast imaging.

In this work, we present a novel approach using a semantic segmentation Convolutional Neural Network (CNN) to quantitatively measure atomic column occupancy. To train the network, we developed a comprehensive library of simulated surface motif models with varying thicknesses (1–10 layers), and randomized column occupancies (specifically targeting both Ce and O vacancies). To ensure robustness against experimental artifacts, the training set incorporated many different defocus conditions, and nine random rotations for each model to account for structural tilt in non-zone axis directions. By utilizing these models, the network is trained to recover structural information from 2D projections, effectively bridging the gap between image intensity and physical occupancy.

Our results demonstrate that the CNN effectively extracts a structural mask from noisy simulated and experimental input images. The developed model achieved training accuracy exceeding 90%, with confusion matrices indicating high precision in predicting atomic occupancy levels. This deep learning framework allows for the identification of oxygen vacancy activity, providing a powerful and scalable tool for interpreting dynamic atomic-scale processes during the oxygen exchange reaction.

[Grad] Morphological Transformation of Ragweed Pollen (Ambrosia artemisiifolia) Following Ozone (O3) Exposure

Nishat Tasnim, Matthew Fraser, and Pierre Herckes

Ragweed pollen (*Ambrosia artemisiifolia*) is a potent aeroallergen well-documented to contribute to IgE-mediated allergic reactions, asthma, and hospital visits. The effect of air pollutants on ragweed pollen has been reported to modify its morphological features, and these changes are hypothesized to correlate with sub-pollen particle (SPP) formation and to alter pollen chemical composition, which, in turn, affects allergenicity and immunology. In this study, the morphological changes in ragweed pollen resulting from exposure to ozone (O3), a major air pollutant, are investigated. The ragweed pollen was exposed to an elevated concentration of ozone levels (~150 ppm) to accelerate the aging process over different time periods (24 hours, 48 hours, and 72 hours) and compared to unexposed pollen. The morphological analysis was performed using Focused Ion Beam/Scanning Electron Microscopy (FIB/SEM; Auriga-Zeiss). The structural disintegration of the outer shell of the pollen (exine) was confirmed with high-resolution imaging. The magnitude of oxidative damage to the pollen exine caused by the high ozone levels was classified into four (4) different categories: deflated, cracked and deflated, deformed, and unidentifiable. The quantitative analysis demonstrated an overall time-dependent increase in signs of oxidative damage to the pollen exine from exposure to high ozone concentrations, with intact grains decreasing from 95 ± 1% at 0 hours to 20 ± 5% at 72 hours, despite minor variability at intermediate time points. A shift toward more damaged pollen was observed, with the highest number of damaged pollen grains recorded at a 72-hour exposure period, corresponding to an increase in deflated, cracked, and deformed pollen grains. These findings demonstrate ozoneinduced oxidative damage to pollen structure, providing insight into the structural changes of pollen in the air and helping elucidate the associated chemical changes. Future work will correlate morphological analysis findings with chemical, cellular, and in vitro immunological analysis to explore the changes affecting inflammation and allergenicity

[Grad] Vibrations and Regeneration: FOXN1 in the Vocal Fold Response to Mechanical Stress

G. Tremonti, T. Riede, K.J. Bussey, Midwestern University, Glendale, AZ

Forkhead-box N1 (FOXN1) is a transcription factor that regulates terminal differentiation of keratinocytes in the basal layer of stratified squamous epithelium. FOXN1 expression increases significantly following injury and has been described as a molecular switch between regenerative (scarless) and reparative (scar-forming) healing based on the skin regeneration phenotype observed in FOXN1^{-}/$^{-}$ mice. Vocal folds are specialized; multilayered tissues adapted for rapid and relatively scarless wound healing. During airflow-induced vibration, vocal folds experience repeated mechanical stress and micro-injury, making them a relevant model for studying injury-responsive regulatory factors such as FOXN1. House mice (Mus musculus) vocalize primarily through whistling, which places minimal mechanical stress on the vocal folds, whereas California deer mice (Peromyscus californicus) produce sound through airflow-induced vocal fold vibration that generates tensile, shear, and impact forces. Here, we examined FOXN1 expression patterns across vocal fold layers and tested the hypothesis that FOXN1 expression is present in tissues exposed to greater mechanical stress. In this study, tissue samples from the larynx, footpad, lung, and kidney from 6 house mice (Mus musculus) and 6 California deer mice (Peromyscus californicus) were evaluated for expression of FOXN1. Tissues were embedded in paraffin using standard histological protocols and cut at a thickness of 5 µm on a standard microtome for slide placement. Slides were treated with a rabbit anti-FOXN1 polyclonal antibody coupled with Alexa Fluor 594. Counterstaining was performed with DAPI. Footpad samples were used as positive controls for FOXN1 expression, while lung and kidney samples were used as negative controls. Immunofluorescent images were obtained using a Stellaris Confocal microscope under constant imaging conditions. Differential interference contrast (DIC) microscopy was used to visualize cell borders of the epithelium, lamina propria, and thyroarytenoid muscle of the vocal folds. Vocal fold tissue from both species was positive for FOXN1 expression. Footpad samples were all positive for FOXN1 expression in the basal layer of epithelium. Both kidney and lung tissue showed low levels of diffuse FOXN1 expression, suggesting potential cross-reactivity of the polyclonal antibody with other FOX proteins. Additionally, all footpad samples from California mice were positive for expression of FOXN1, confirming reactivity of the chosen antibody in this species; given the large divergence between the Cricetid (Peromyscus spp.) and Murid (Mus spp.) family of rodents, this is consistent with FOX proteins being highly conserved. FOXN1 expression was observed in vocal fold tissue of both species, suggesting a potential role for FOXN1 in epithelial responses to mechanical stress and micro-injury. Ongoing analyses using a CellProfiler colocalization pipeline will quantify nuclear and cytoplasmic FOXN1 expression patterns in the vocal fold epithelium, lamina propria fibroblasts, and myofibers of both species to further characterize its role in stress- and injury-responsive regulation.

[UG] 3D Reconstructions of Lung Tissue Microarchitecture from Serial H&E Sections and Integration with Spatially-Resolved Transcriptomic Data

Maddox Turner, Banovich Lab

Understanding the three-dimensional organization of lung tissue is critical for characterizing developmental trajectories and disease progression in pulmonary fibrosis (PF). Conventional histological analysis relies on two-dimensional sections, which limit full spatial context and the ability to capture volumetric tissue architecture. Here we present a Python pipeline for 3D reconstruction of lung tissue microarchitecture from serially sectioned hematoxylin & eosin (H&E)-stained tissue microarrays (TMAs). The pipeline performs automated TMA core cropping, serial image registration across the Z plane, and the construction of a meta-tensor object representing the full 3D tissue volume. This volumetric representation is subsequently co-registered to Xenium ST data, enabling spatially resolved gene expression to be anchored within 3D context. Preliminary lumen segmentation and morphological analysis demonstrate the feasibility of extracting luminal features directly from the 3D H&E model, with transcriptomic profiling of lumen-associated regions providing an initial genomic readout of microarchitectural compartments. This pipeline and toolset aims to support ongoing studies of lung development and PF progression by enabling correlative 3D histology and spatial transcriptomics at the TMA scale

[UG] Histological analysis of graft rejection within macroencapsulated allogeneic and xenogeneic rat models

Tanush Varma, Tuhfah Norris, Jessica Weaver

Over 9.5 million people worldwide live with Type 1 Diabetes (T1D), a condition that remains one of the top ten causes of death globally.[1] While daily insulin administration is the current clinical standard, it often fails to prevent life-threatening secondary complications and lacks the permanence of a definitive cure. Cell therapy, such as allogeneic islet transplantation, has demonstrated feasibility to functionally cure T1D by restoring endogenous insulin signaling. However, the success of allogeneic islet transplantation is currently hindered by the requirement for chronic systemic immunosuppression. To address this, we investigate complex geometry hydrogel microencapsulation devices in a spiral configuration, designed to provide a semi-permeable barrier, facilitating the exchange of oxygen and nutrients through the hydrogel while preventing immune cells from infiltrating into the capsule. We utilized this model to evaluate the kinetics of graft rejection across both allogeneic and xenogeneic rat models to examine the influence of transplant sites, vascularization, and cell density. Histological analysis was employed to characterize the physiological response and biocompatibility of these constructs using Hematoxylin and Eosin (H&E) staining to visualize immune cell infiltration, and Masson's Trichrome to assess foreign body responses through collagen deposition. Overall, we hope to understand the influence of transplantation factors such as transplant sites, vascularization, and cell density on macrencapsulation through histology.

[UG] Neuroimmune Deficits of Early Life Stress: Insights from Fluorescence Microscopy

Jakob Villarreal, Lindsay Halladay

Early life stress (ELS) is a known risk factor for developing a multitude of neuropsychiatric and behavioral disorders in adulthood, especially when experienced in conjunction with later-life stress. Yet, the neurobiological mechanisms explaining these clinical outcomes remain unresolved. Recent evidence suggests that ELS' impacts on neuroimmune activity may mediate its behavioral deficits, but the contributions of individual neuroimmune system components to these deficits have not been adequately distinguished. With a mouse model of ELS, maternal separation with early weaning (MSEW), that consistently produces aberrant socioemotional behavior, we explored ELS' and acute stress' individual and synergistic effects on three neuroimmune components, the blood-brain barrier (BBB), microglia, and astrocytes, known for their capacity for behavioral modulation. In particular, we quantified various morphological and immunofluorescent parameters reflective of these components' activity using immunohistochemical staining and fluorescence microscopy.

To model ELS, MSEW mice (C57BL/6J) were subjected to 4h maternal separations from postnatal days (PD) 2-5, 8h separations on PD6-16, and early weaning on PD17. Non-stressed controls (NS) were kept with dams and weaned on PD21. During adulthood, half of all MSEW/NS adult mice underwent a two-day forced swim (FS) procedure, eliciting an acute stress response. All mice were injected with Evans Blue (EB), a fluorescent tracer that only enters the brain upon BBB disruption (a precipitator of aberrant immunological signaling), and brains were extracted. Tissue was serially sectioned and immunostained for one of the following protein marker combinations: Iba-1 (microglia), GFAP (astrocytes), or tight junction proteins (TJP) Occludin and Claudin-5 (BBB). Microglial density and mean fluorescent intensity (MFI) above background were quantified using cellSens (Olympus) automated thresholding of 20x images, and manually screened for “phagocytic” and “ameboid” morphological types based on a priori categorization. Astrocyte (captured in 60x Z-stacks) morphological features and complexity were measured using semi-automated tracing of individual cell processes with the FIJI SNT plugin and Sholl Analysis. BBB integrity was measured via calculation of EB MFI and TJP MFI in cellSens, as well as TJP structural features (average length, area fraction, etc.) using the ImageJ AnalyzeSkeleton Plugin applied to 60x Maximum-Z projections of stained tissue.

Acutely-stressed MSEW mice demonstrated increased BBB permeability (EB MFI) and correspondent TJP downregulation, with decreased Claudin-5 area fractions and MFI. Likewise, all MSEW mice showed increased “ameboid”, activated microglia morphologies, with no change in total microglial density or immunoreactivity. They also demonstrated decreased astrocyte process length and complexity compared to NS controls, with unclear effects of acute stress.

ELS appears to alter baseline activity of microglia and astrocytes, with potential ramifications for their response to acute stressors. In turn, these alterations could play a role in the acute stress-induced BBB leakage seen in MSEW mice. Taken together, our findings support the hypothesis that ELS "primes" the neuroimmune system via increasing its baseline activity and response to subsequent psychological challenges. The findings also provide a foundation for more thorough characterization of the microglial and astrocyte functional changes introduced by ELS and perturbational studies linking these changes to behavioral deficits.

SPONSORS

The Arizona Imaging and Microanalysis Society is grateful for generous support from sponsors.

MSA Microscopy Society of America

ARIZONA DEPARTMENT OF HEALTH SERVICES
Arizona Biomedical Research Centre

MAS Microanalysis Society

Platinum Corporate Sponsors

ThermoFisher SCIENTIFIC

HITACHI Inspire the Next

Nikon

CAMECA SCIENCE & METROLOGY SOLUTIONS
AMETEK

nanoScience Instruments

Gold Corporate Sponsors

NCI
a Thomas Scientific, LLC company

BRUKER

EVIDENT™
OLYMPUS

Direct Electron®

MICROSCOPY INNOVATIONS LLC

JEOL

TESCAN
PERFORMANCE IN NANOSPACE

Electron
Microscopy
Sciences
POWERED BY biolyst SCIENTIFIC

ZEISS